Eur. Phys. J. C 32, 221–228 (2004)
Digital Object Identifier (DOI) 10.1140/epjc/s2003-01357-3

THE EUROPEAN PHYSICAL JOURNAL C

A measurement of Λ polarization in inclusive production by Σ^- of 340 GeV/c in C and Cu targets

The WA89 Collaboration

M.I. Adamovich[8,†], Yu.A. Alexandrov[8,a], S.P. Baranov[8,a], D. Barberis[3], M. Beck[5], C. Bérat[4], W. Beusch[2], M. Boss[6], S. Brons[5,b], W. Brückner[5], M. Buénerd[4], Ch. Busch[6], Ch. Büscher[5], F. Charignon[4], J. Chauvin[4], E.A. Chudakov[6,c], U. Dersch[5], F. Dropmann[5], J. Engelfried[6,d], F. Faller[6,e], A. Fournier[4], S.G. Gerassimov[8,f], M. Godbersen[5], P. Grafström[2], Th. Haller[5], M. Heidrich[5], E. Hubbard[5], R.B. Hurst[3], K. Königsmann[5,g], I. Konorov[5,8,f] N. Keller[6], K. Martens[6,h], Ph. Martin[4], S. Masciocchi[5,i], R. Michaels[5,c], U. Müller[7], H. Neeb[5], D. Newbold[1], C. Newsom[j], S. Paul[5,f], J. Pochodzalla[5,k] I. Potashnikova[5], B. Povh[5], R. Ransome[l], Z. Ren[5], M. Rey-Campagnolle[4,m], G. Rosner[7], L. Rossi[3], H. Rudolph[7], C. Scheel[n], L. Schmitt[7,f], H.-W. Siebert[6], A. Simon[6,g], V. Smith[1,o], O. Thilmann[6], A. Trombini[5], E. Vesin[4], B. Volkemer[7], K. Vorwalter[5], Th. Walcher[7], G. Wälder[6], R. Werding[5], E. Wittmann[5], M.V. Zavertyaev[8,a]

[1] University of Bristol, Bristol, United Kingdom
[2] CERN, 1211 Genève 23, Switzerland
[3] Genoa Univ./INFN, Dipt. di Fisica, 16146 Genova, Italy
[4] Grenoble ISN, 38026 Grenoble, France
[5] Max-Planck-Inst. für Kernphysik, Postfach 103980, 69029 Heidelberg, Germany
[6] Universität Heidelberg, Physikalisches Institut, 69120 Heidelberg, Germany[p]
[7] Universität Mainz, Inst. für Kernphysik, 55099 Mainz, Germany
[8] Moscow Lebedev Physics Inst., 117924, Moscow, Russia

Received: 2 April 2003 /
Published online: 27 November 2003 –

Abstract. We have measured the polarization of Λ hyperons produced inclusively by a Σ^- beam of 340 GeV/c momentum in nuclear targets. From a sample of 9.5 millions of identified Λ decays, polarizations were determined in the range $x_F > 0.1$ and $p_t \leq 1.6$ GeV/c. The polarization w.r.t. the production normal is mainly positive for $x_F \geq 0.3$. At fixed values of x_F, it increases with p_t to a maximum between p_t=0.5 and p_t=1 GeV/c , and then decreases to zero or even negative values, in sharp contrast to the plateau above p_t=1 GeV/c observed in inclusive Λ production by protons.

1 Introduction

For more than 25 years [1] it has been well known that hyperons produced inclusively by unpolarized hadron beams of momenta around and beyond 100 GeV/c are polarized transverse to the production plane. In particular, the polarization of Λ particles produced by protons has been investigated in great detail using proton beams of momenta between 300 and 800 GeV/c at Fermilab [1–5] and

[a] supported by Deutsche Forschungsgemeinschaft, contract number DFG 436 RUS 113/465/0-2(R), and Russian Foundation for Basic Research under contract number RFFI 00-02-04018
[b] Now at TRIUMF, Vancouver, B.C., Canada V6T 2A3
[c] Now at Thomas Jefferson Lab, Newport News, VA 23606, USA
[d] Now at Instituto de Fisica, Universidad Autonoma de San Luis Potosi, S.L.P. 78240 Mexico
[e] Now at Fraunhofer Inst. für Solare Energiesysteme, 79100 Freiburg, Germany
[f] Now at Technische Universität München, Garching, Germany
[g] Now at Fakultät für Physik, Univ. Freiburg, Germany
[h] Now at Department of Physics and Astronomy, SUNY at Stony Brook, NY 11794-3800, USA
[i] Now at Max-Planck-Institut für Physik, München, Germany
[j] University of Iowa, Iowa City, IA 52242, USA
[k] Universität Mainz, Institut für Kernphysik, Germany
[l] Rutgers University,Piscataway, NJ 08854, USA
[m] permanent address: CERN, 1211 Genève 23, Switzerland
[n] NIKHEF, 1009 DB Amsterdam, The Netherlands
[o] supported by the UK PPARC
[p] supported by the Bundesministerium für Bildung und Forschung, Germany, under contract numbers 05 5HD15I, 06 HD524I and 06 MZ5265
[†] *deceased*

at CERN [6], and also at the ISR [7,8]. It turned out the Λ polarization is almost independent of the beam momentum and increases almost linearly with p_t up to a plateau at about 1 GeV/c . The height of this plateau increases with x_F and the polarization reaches values well above 20% at large x_F and p_t. The polarization is negative, i.e. opposite to the production plane normal $\hat{n} \propto \hat{p}_{\rm beam} \times \hat{p}_\Lambda$, where $\hat{p}$ denotes the beam particle and Λ directions. (p_t is the Λ momentum component transverse to the beam particle direction and x_F is the longitudinal Λ momentum in the beam particle – target nucleon CMS divided by its maximum possible value, viz. $x_F = 2p_L^{CMS}/\sqrt{s}$).

Λ polarization has also been found in production by neutrons of 40–70 GeV/c at Serpukhov [9], with values similar to those observed in the proton beams.

The Λ polarization has also been measured in a π^- beam of 230 GeV/c at CERN, where it was found to be small and of the same sign as in production by protons [10], and in a K^- beam of 176 GeV/c at Fermilab, where it was found to be much larger than the polarization in production by protons and to be of opposite sign [11].

Other hyperons produced inclusively in proton beams are polarized as well, Ξ^- and Ξ^0 with the same sign [3,12–14] and $\Sigma^\pm$ with the opposite sign [15–18] relative to the Λ polarization. Ω^-, on the other hand, are produced unpolarized [19]. Of the antihyperons, $\overline{\Lambda}$ are produced unpolarized [2,4,5,20] while $\overline{\Sigma}^-$ and $\overline{\Xi}^+$ show polarizations similar to those of the corresponding hyperons [17,21].

This complex behaviour so far is not fully understood. The signs of the hyperon polarizations can be reproduced qualitatively through the Lund model of Andersson, Gustafson, Ingelman, and Sjostrand [22] or the recombination model of DeGrand and Miettinen [23] in which the valence quark overlap between beam projectile and produced hyperons is important. The nonzero polarizations of the antihyperons $\overline{\Sigma}^-$ and $\overline{\Xi}^+$, however, remain unexplained. Recently, polarizing quark fragmentation functions have been derived from the Λ and $\overline{\Lambda}$ polarization data in inclusive production by protons [24], but no predictions on polarizations in other hadronic production processes have been made. For reviews of the experimental and theoretical situation see for instance [25–29].

Further insights into the role of the valence quark content of the beam particle may arise from a new class of hyperon polarization experiments which use high-intensity beams of Σ^-. We present here the results of a polarization study based on a sample of 9.5 million identified $\Lambda \to p\pi^-$ decays produced by a Σ^- beam of 340 GeV/c mean momentum in copper and carbon targets. These data were recorded in 1993 and 1994 in the CERN hyperon beam experiment WA89. A preliminary study of Λ, $\overline{\Lambda}$, Σ^+ and Ξ^- polarizations based on a smaller sample recorded in 1991 in the same experiment has already been published [31].

In an extension of the DeGrand and Miettinen model, Yamamoto, Kubo and Toki predict negative polarization for Λ produced in a Σ^- beam [32], as in production by protons. Liang and Boros also predict negative, but small polarization [33].

2 Hyperon beam and experimental apparatus

The hyperon beam was derived from an external proton beam of the CERN-SPS at 450 GeV/c momentum, which was deflected downward by an angle of 7 mrad before hitting the hyperon production target, which consisted of Be rods of diameter 2mm and total length 400mm. A magnetic channel selected charged secondaries from this target at production angles of less than 1 mrad. This ensured that the hyperons in the secondary beam had a negligible polarization. Three 2.4 T dipole mgnets of 8.4 Tm bending power each bent the secondary beam up/up/down in steps of 7 mrad, thereby restoring the direction of an unbent beam going through the center of the apparatus. The angular acceptance of the beam was defined by a set of brass and tungsten collimators. At the collimator exit, the mean beam angle and its full width were $(+0.5 \pm 1.0)$ mrad horizontally and $(+0.5 \pm 0.5)$ mrad vertically w.r.t. the symmetry axis of the experiment. The mean beam momentum was 345 GeV/c and 330 GeV/c in the beam periods 1993 and 1994, respectively and the momentum spread was $\sigma(p)/p \approx 9\%$.

The secondary beam was directed onto the experiment target, which was situated 16m downstream of the hyperon production target. At the experiment target, the beam had a width of 3 cm and a height of 1.7 cm and consisted of π^-, K^-, Σ^- and Ξ^- in the ratio 2.3 : 0.025 : 1 : 0.008. A transition radiation detector (TRD) made up of 10 MWPCs interleaved with foam radiators allowed π^- to be suppressed at the trigger level. Typically, about $1.8 \cdot 10^5$ Σ^- and $4.2 \cdot 10^5$ π^- were delivered to the target during one SPS-spill, which had an effective length of about 1.5 s. A detailed description of the hyperon beam can be found in [34].

The experiment target consisted of one copper and three carbon blocks arranged in a row along the beam, with thicknesses corresponding to 0.026 and three times 0.0083 interaction lengths, respectively. The copper block was positioned upstream of the carbon blocks and the block-to-block distance was 2 cm. Microstrip detectors upstream and downstream of the target allowed the tracks of the incoming beam particle and of the charged particles produced in the target blocks to be measured. The momenta of the incoming beam particles, however, could not be measured individually.

The target was positioned 14m upstream of the centre of the Omega spectrometer magnet [35] so that a field-free decay region of 10m length was provided for hyperon and K_S decays. The Omega magnet had circular poleshoes of diameter 4.0 m, with a vertical distance of 1.8 m. It provided a field integral of 7.5 Tm. Tracks of charged particles were measured inside the magnet and in the field-free regions immediately upstream and downstream by MWPCs and drift chambers, with a total of 130 planes. The momentum resolution achieved was $\sigma(p)/p^2 \approx 10^{-4}$ $({\rm GeV}/c)^{-1}$.

Downstream of the spectrometer, a ring-imaging Cherenkov detector, an electromagnetic calorimeter and a hadron calorimeter were placed. In the analysis presented here, only the lead-glass calorimeter was used to identify $\Sigma^0 \to \Lambda\gamma$ decays. It is described in [36].

The main trigger selected about 25% of all interactions, using multiplicities measured in microstrip counters upstream and downstream of the target, and in scintillator hodoscopes and MWPCs behind the Omega magnet. Correlations between hits in different detectors were used in the trigger to increase the fraction of events with high-momentum particles, thus reducing background from low-momentum pions in the beam. In addition, a reduced sample of beam triggers was recorded for trigger calibration purposes. The results presented in this article are based on 200 million events recorded in 1993 and 1994.

3 Selection of Λ decays

Each accepted event had to have a single beam track reconstructed in the silicon microstrip counters upstream of the experiment target, and an interaction vertex containing at least two outgoing charged tracks reconstructed in the microstrip counters downstream of the target. To suppress interactions of neutrons and Λ from Σ^- and Ξ^- decays upstream of the experiment target, the beam track had to have a transverse distance to the reconstructed interaction vertex of less than 500 μm. To suppress interactions of particles scattered from the collimator walls, the position/direction correlation for beam particles coming directly from the proton target had to be fulfilled. For a given beam direction in one projection, the requirement was a deviation of less than 5mm from the mean beam impact, which corresponds to a 3σ cut.

Λ candidates then were selected from all pairs of positive and negative tracks which formed a vertex in the decay zone between the target region and the Omega magnet. The tracks had to have elements reconstructed in the drift chambers located in the field-free region upstream of the Omega magnet. The distance between the two tracks at the decay point had to be smaller than 3 mm. Background from e^+e^-pair production was suppressed by requiring that the daughter CMS momenta transverse to the Λ direction of motion be greater than 10 MeV/c.

Figure 1 shows the mass distributions for Λ candidates with $0.1 < x_F < 0.2$ and $0.8 < x_F < 0.9$, respectively. The r.m.s. of the Λ mass peaks can be parametrized as $\sigma_m^2 = a^2 + (b \cdot p_\Lambda)^2$, with a, the contribution from multiple scattering being ≈ 1.5 MeV/c^2 and $b \cdot p_\Lambda$, the contribution from coordinate measurement errors being ≈ 1.6 MeV/c^2 at 100 GeV/c .

Λ candidates had to be within $\pm 2\,\sigma_m$ of the Λ mass. The background/signal ratio within this signal window decreases rapidly from 0.10 at $x_F < 0.2$ and $p_t < 200\,MeV/c$ to 0.05 with increasing x_F and p_t, and rises to 0.07 at $x_F > 0.8$. Below $x_F = 0.1$, the signal/background ratio deteriorates rapidly and we decided to reject this kinematical region.

After subtraction of a linear background taken from "side windows" inside $\pm$ 24 MeV/c^2, a sample of 9.5 million Λ decays remained in the range $0.1 < x_F < 1$. It should be noted that this background subtraction also removed the contamination from misidentified $K_S \to \pi^+\pi^-$ decays.

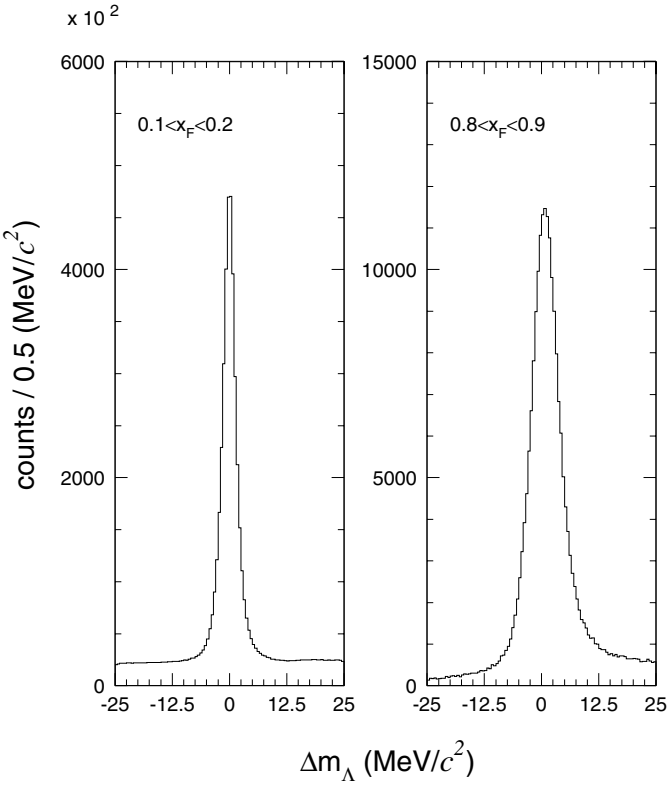

Fig. 1. Δm_Λ, the difference between the reconstructed $p\pi^-$ effective mass and the Λ mass

4 Polarization analysis

The polarizations were measured w.r.t. the direction of the production normal $\hat{n} \propto \hat{p}_{\rm beam} \times \hat{p}_\Lambda$, using the relation $f(cos\vartheta_p^*) \propto 1 + A \cdot cos\vartheta_p^*$, where $A = P_\Lambda \cdot \alpha_\Lambda$ is the product of the Λ polarization and decay parameter and ϑ_p^* is the angle between the production normal and the direction of the decay proton in the Λ-CMS. $\alpha_\Lambda = 0.642$ is the Λ decay parameter [37]. The beam particle direction $\hat{p}_{\rm beam}$ was measured individually. The polarizations were determined in 8·8 bins of x_F and p_t, as listed in Tables 1 and 2 (the two bins at the largest x_F and p_t values were merged to retain an acceptable sample size).

We used a coordinate system with the symmetry axis of the experiment as the x-direction, which practically coincided with the mean beam direction. The y-axis pointed horizontally to the left, looking downstream, and the z-axis vertically upwards (see Fig. 2). In this geometry, the production normal was confined to the y-z plane and had an azimuth $\varphi_n = \varphi_\Lambda + 90^o$.

4.1 Bias cancelling

Biases resulting from unrecognized apparatus asymmetries are the main cause for worry in any polarization measurement. For instance, the Omega magnet bent positively/negatively charged particles to the left/right, thereby introducing a strong acceptance bias in favour of pion emission to the left (for proton emission, the effect is much

Table 1. Polarization results I. The statistics of the Λ signal is after background subtraction. p_t is in units of GeV/c

sample	Λ sample		mean	mean	polarization	
no.	signal	bgrd.	x_F	p_t	[%]	$\chi^2_{\rm sect}$
1	276417	29071	0.15	0.13	-0.8 ± 1.2	0.4
2	665082	55130	0.15	0.30	-0.2 ± 1.3	10.3
3	652211	42700	0.15	0.50	-0.3 ± 1.1	1.4
4	448564	24220	0.15	0.69	-0.8 ± 1.1	1.0
5	262506	12073	0.15	0.89	-1.8 ± 1.2	1.6
6	136695	5570	0.15	1.09	0.5 ± 1.3	3.8
7	68685	2636	0.15	1.29	-1.7 ± 2.9	12.3
8	61937	2220	0.15	1.66	0.3 ± 1.5	0.5
9	249919	12465	0.25	0.13	-0.3 ± 1.1	0.1
10	611542	26838	0.25	0.31	0.5 ± 1.2	8.4
11	637737	25001	0.25	0.50	0.6 ± 1.2	7.0
12	429295	15514	0.25	0.69	-0.3 ± 1.4	11.1
13	222666	7891	0.25	0.89	-2.1 ± 1.2	0.9
14	101820	3702	0.25	1.09	-1.3 ± 1.3	1.4
15	45745	1641	0.25	1.29	-2.9 ± 2.6	6.3
16	38482	1505	0.25	1.66	-3.3 ± 1.8	0.4
17	187875	7426	0.35	0.13	2.1 ± 1.2	4.7
18	447107	16346	0.35	0.31	3.6 ± 1.1	1.1
19	483199	15912	0.35	0.50	3.5 ± 1.4	12.7
20	345614	11346	0.35	0.69	2.3 ± 1.1	5.0
21	184348	6209	0.35	0.89	0.6 ± 1.2	0.3
22	80707	2910	0.35	1.09	0.3 ± 1.4	1.4
23	32994	1268	0.35	1.29	-3.7 ± 1.8	2.3
24	23422	1102	0.35	1.64	-5.1 ± 2.1	0.3
25	127887	5147	0.45	0.13	3.2 ± 1.3	3.0
26	300335	11418	0.45	0.31	5.9 ± 1.1	1.0
27	328100	11686	0.45	0.50	8.2 ± 1.1	2.3
28	242562	8646	0.45	0.69	7.2 ± 1.1	0.6
29	133854	4851	0.45	0.89	4.9 ± 1.3	0.1
30	59588	2275	0.45	1.08	0.8 ± 1.5	1.9
31	23173	1003	0.45	1.29	-1.1 ± 2.1	1.7

Table 2. Polarization results II

sample	Λ sample		mean	mean	polarization	
no.	signal	bgrd.	x_F	p_t	[%]	$\chi^2_{\rm sect}$
32	15368	748	0.45	1.62	-1.4 ± 2.5	0.0
33	85256	3799	0.55	0.13	3.1 ± 1.4	4.9
34	190750	8256	0.55	0.30	8.4 ± 1.2	0.5
35	198054	8492	0.55	0.50	9.7 ± 1.2	4.6
36	149519	6296	0.55	0.69	11.2 ± 1.2	1.2
37	85203	3766	0.55	0.89	7.1 ± 1.4	0.8
38	38217	1773	0.55	1.09	7.1 ± 1.7	0.2
39	14975	813	0.55	1.28	-2.7 ± 2.5	3.3
40	9360	602	0.55	1.62	-7.5 ± 3.1	0.9
41	62066	3030	0.65	0.13	3.4 ± 1.5	1.4
42	118887	6009	0.65	0.30	7.7 ± 1.3	0.2
43	107882	5746	0.65	0.50	12.9 ± 1.3	5.5
44	77757	4165	0.64	0.69	13.0 ± 1.4	4.3
45	44959	2380	0.64	0.89	12.4 ± 1.6	0.7
46	20632	1205	0.64	1.09	11.2 ± 2.1	1.4
47	8110	548	0.64	1.28	6.8 ± 3.2	1.0
48	4765	371	0.64	1.61	3.6 ± 4.2	0.3
49	48525	2206	0.75	0.13	5.3 ± 1.6	0.1
50	68878	3804	0.75	0.30	8.6 ± 1.5	0.4
51	51651	3240	0.74	0.49	12.2 ± 1.6	5.4
52	33192	2168	0.74	0.69	15.3 ± 1.8	1.5
53	18617	1299	0.74	0.89	15.5 ± 2.2	4.9
54	8434	683	0.74	1.09	12.6 ± 3.2	3.0
55	3396	293	0.74	1.28	6.5 ± 4.7	0.3
56	1946	223	0.74	1.60	-0.9 ± 6.3	1.5
57	34314	1924	0.86	0.12	1.7 ± 1.8	0.2
58	37454	2493	0.86	0.29	5.6 ± 1.7	2.6
59	22938	1796	0.86	0.49	11.8 ± 2.0	3.6
60	12808	1147	0.86	0.69	17.4 ± 2.6	1.5
61	6715	673	0.85	0.89	20.7 ± 3.5	0.0
62	3135	370	0.85	1.09	14.8 ± 5.0	0.3
63	2026	318	0.86	1.42	-9.1 ± 6.4	3.7

smaller owing to the larger momenta and smaller decay angles of the protons). If not properly taken into account, this acceptance bias would translate into a positive polarization bias for Λ emitted upwards and a corresponding negative polarization bias for Λ emitted downwards.

In order to cancel apparatus biases, we adopted the following procedure: to determine the polarization in a given interval of x_F and p_t we subdivided that x_F/p_t sample into subsamples corresponding to 12 sectors of 30° in φ_Λ as shown in Fig. 2. The polarizations determined in each sector then were averaged to obtain bias cancellation. Let us suppose there is a bias in the Λ reconstruction such that for π^- emission to the left, i.e. $\varphi_\pi \approx 0^0$, the reconstruction efficiency is larger than for π^- emission to the right, $\varphi_\pi \approx 180^0$. This will result in a **positive** polarization bias for Λs emitted **upwards** ($\varphi_\Lambda \approx +90^0$), and a **negative** polarization bias for Λs emitted **downwards** ($\varphi_\Lambda \approx -90^0$), and these biases will cancel each other. This holds for all biases – **known and unknown**.

In each sector, the polarization was determined by two methods:
– calculating the asymmetry

$$a(\cos\vartheta) = (n(\cos\vartheta) - n(-\cos\vartheta))/(n(\cos\vartheta) + n(-\cos\vartheta))$$

in 10 bins of $0 < \cos\vartheta < +1$ and then determining A from a fit to $a(\cos\vartheta) = A \cdot \cos\vartheta$
– calculating A directly from the relation $2A = (n(\cos\vartheta > 0) - n(\cos\vartheta < 0))/(n(\cos\vartheta > 0) + n(\cos\vartheta < 0))$.
To be bias-free, the first method requires only

$$\epsilon(cos\vartheta_p^*) = \epsilon(-cos\vartheta_p^*)\,,$$

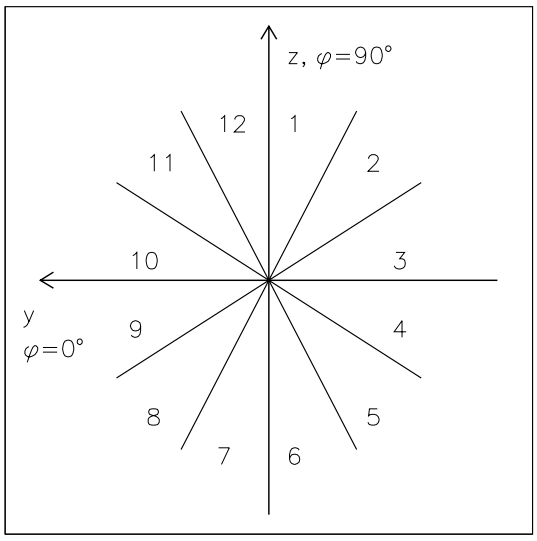

Fig. 2. Definition of azimuth angles φ and numbering of Λ azimuth sectors

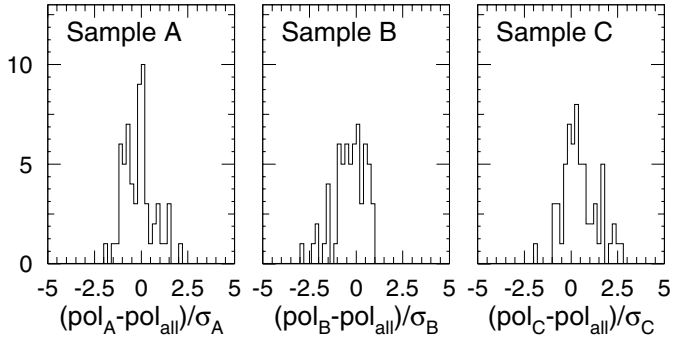

Fig. 3. Deviations of the polarizations measured in sector subsamples from the polarization averaged over all sectors. Each plot has 63 entries corresponding to the 63 x_F/p_t samples

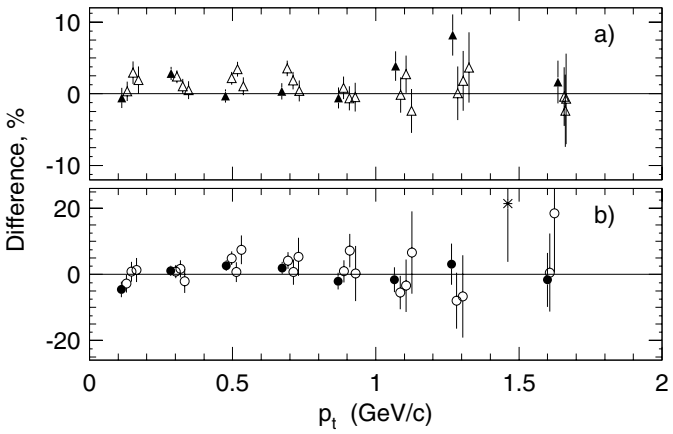

Fig. 4. The difference $pol_C - pol_B$ (in units of %) as a function of p_t for $x_F < 0.5$ (top) and $x_F > 0.5$ (bottom). At a given value of p_t, the full symbols correspond to the lowest bin in x_F and the open symbols are staggered to the right with increasing x_F for clarity. The value corresponding to x_F/p_t bin no. 63 is indicated by a cross

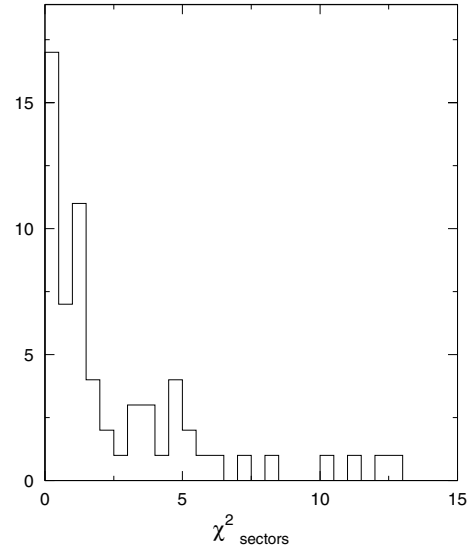

Fig. 5. Distribution of $\chi^2_{\rm sectors}$. The plot has 63 entries corresponding to the 63 x_F/p_t samples. There are no overflows

while the second method requires a constant efficiency over the full range of $cos\vartheta^*_p$. Both methods gave the same results within the statistical errors, with no apparent bias. We used the results from the first method.

As a check for the reliability of the bias-cancelling, we averaged the polarizations in three subsamples of four φ_Λ sectors each, sample A comprising Λ azimuths inside $\pm 30^0$ to the vertical (sectors 1,6,7,12), sample B comprising Λ azimuths inside $\pm 15^0$ to the diagonals (sectors 2,5,8,11), and sample C comprising Λ azimuths inside $\pm 30^0$ to the horizontal (sectors 3,4,9,10). If, for instance, the large left/right acceptance bias resulting from the horizontal bending of the tracks was not fully cancelled, we would expect the polarizations measured in sample A to differ systematically from the polarizations in samples B and C. Figure 3 shows the distributions of $(pol_i - pol_{\rm all})/\sigma_i$, where $i = A, B, C$. pol_i is the polarization measured for subsample i in a given x_F/p_t bin, σ_i is its statistical error and $pol_{\rm all}$ is the polarization averaged over subsamples A,B and C. Thus each plot contains 63 entries for the 63 different x_F/p_t bins. The observed r.m.s. values of the distributions are 0.81, 0.84 and 0.93, in agreement with what we would expect from purely statistical fluctuations, viz. $\sigma = \sqrt{2/3} = 0.82$. The mean values of the distributions are -0.15±0.10, -0.35±0.11 and +0.47±0.12 for A, B and C, respectively, which may indicate incomplete bias-cancelling.

In Fig. 4 we show the difference $pol_C - pol_B$ as a function of p_t for $x_F < 0.5$ (a) and $x_F > 0.5$ (b). At small x_F and p_t, where the statistics is large, this difference has a non-zero value of about +0.01. At high x_F or p_t, a shift of this magnitude is masked by the larger statistical errors. Since we have no means to decide whether incomplete bias-cancelling in sample C or rather in sample B causes this effect, we do not add a systematic shift to the polarizations, but a systematic error of 0.01 (rms).

Figure 5 shows the distribution of

$$\chi^2_{\rm sectors} = \sum_i (pol_i - pol_{\rm all})^2/\sigma_i^2$$

$\chi^2_{\rm sectors}$ is also listed in Tables 1 and 2.

While the mean value 2.64 is not far from the value 2 expected for purely statistical fluctuations, we note a few large values up to 12. The larger values all occur in samples at low x_F, but no preference for low or high p_t is observed. As a further precaution against the possibility of biases not fully cancelled, we increased the statistical errors of the polarizations by a factor $\sqrt{\chi^2_{\rm sectors}/2}$, for $\chi^2_{\rm sectors} > 6$. (This method is used by the Particle Data Group in averaging results from different experiments [37]).

We have also split our samples into subsamples of equal size in each x_F/p_t bin, with the beam direction to the right/left or up/down respectively, and for long/short Λ decay lengths. Comparison of these subsamples revealed no systematic differences.

4.2 Beam contaminations

In the following, we investigate possible effects of beam contaminations on our results.

12% of the beam particles accepted in the trigger are fast π^-, which have the same momentum and angular distributions as the Σ^- and were not rejected by the TRDs (note without rejection by the TRDs, the π^-/Σ^- ratio in the beam is 2.3). In our experiment, we found the ratio of the cross sections for Λ production by π^- and by Σ^- to decrease from 0.3 at $x_F \approx 0.15$ to 0.1 above $x_F \approx 0.4$ [38]. The polarization of Λ produced in a π^- beam of 230 GeV/c was found to be between 0 and -0.1 [10]. Therefore the correction for the pion contamination is negligible.

The beam also contains an admixture of 2.2% of K^-. The cross section ratio $\sigma_{K^-\to\Lambda}/\sigma_{\pi^-\to\Lambda}$ for Λ production by K^- and by π^- has been measured in a 200 GeV/c beam [39] and the ratio $\sigma_{\pi^-\to\Lambda}/\sigma_{\Sigma^-\to\Lambda}$ has been measured in our experiment (see above). Combination of these experimental ratios yields $\sigma_{K^-\to\Lambda}/\sigma_{\Sigma^-\to\Lambda} = 0.4-0.6$ in the range of $0.2< x_F <0.8$. Thus, about 1% of all Λ in our sample were produced by K^-. The polarization of Λ produced by K^- of 176 GeV/c momentum is large and positive, attaining values of +0.6 at a mean x_F of 0.57 and a mean p_t of 0.85 GeV/c [11]. Even this large polarization would produce a shift of only about 0.6% in our measured polarizations, which is small compared to our experimental errors in this kinematic region.

Our sample of Λ decay candidates also contains Λ particles from Ξ^- decays. Most of these decays fall into the acceptance of the spectrometer and then are easily identified by the $\Lambda\pi^-$ mass peak.

The beam contains a fraction of 1.2% of Ξ^-. The kinematics of $\Xi^- \to \Lambda\pi^-$ decay confine Λ particles from the decays of these beam Ξ^- to the region of large x_F and small p_t. In samples 49 and 57 (see Table 2) the fraction of Λ particles from identified Ξ^- decays is 6% or 10%, respectively. This is negligible, given the errors of the measured polarizations in these samples.

The fraction of Λ particles from the decays of Ξ^- produced in the target is lower, it decreases linearly from 5% at low x_F to 1% at high x_F, and is almost independent of p_t. From the analysis of our 1991 data [31], we know that Ξ^- produced in Σ^- interactions have negative polarizations, which reach about 10% at large x_F and p_t. This polarization is almost fully transmitted to the daughter Λ with a dilution factor $d = (1 + 2\gamma_\Xi)/3 = 0.93$. The resulting corrections, however, are negligible.

We conclude that corrections for the beam contaminations are not needed.

5 Results

The polarization results for all x_F/p_t bins are listed in Tables 1 and 2. The errors quoted are the statistical and systematic errors added quadratically. In Fig. 6 we show the polarizations as a function of x_F in fixed intervals of p_t with the mean value of p_t indicated in each plot. The sign of the polarization is positive except maybe for the highest values of p_t. Below $p_t \approx 0.6$, the polarization reaches a plateau at $x_F \approx 0.6$, with the height of the plateau increasing with p_t. From $p_t \approx 0.6$ to $p_t \approx 1.2$ GeV/c , the polarization increases up to $x_F = 1$, reaching 20% at $p_t = 0.9$ GeV/c . Above $p_t = 1.2$ GeV/c , the polarization breaks down, being consistent with zero within the experimental errors.

In Fig. 7 we show the polarizations as a function of p_t in fixed intervals of x_F. Above $x_F \approx 0.4$, we see the polarization rising with p_t to a peak at around $p_t = 0.6$, and then dropping back to zero or even negative values. Such a behaviour has never before been observed in inclusive hadronic production of hyperons.

We also looked for a possible dependence of the polarization on the target nuclei. In order to increase the sensitivity of the Cu/C comparison, we have reduced the number of x_F/p_t bins from 63 to 15. Figure 8 shows the polarizations separately for the Cu and C target, as a function of x_F for the p_t-ranges (from left to right) 0–0.4, 0.4–0.8, 0.8–1.2, >1.2. We do not see a systematic Cu/C difference.

6 Discussion

One striking feature of our results is the mostly *positive* sign of the polarization, which is opposite to what has been observed in Λ production by protons or neutrons, and the same as in production by K^-. The sign is opposite to the predictions of refs. [32, 33].

Our preliminary result from the 1991 data, reported in [31], was for an average $x_F = 0.3$. The measured polarizations were *negative*, but only the values at $p_t = 1.0$ and 1.3 differ significantly (by ≈3 st.dev.) from zero. In the second and third plot of Fig. 7, which are for an average $x_F = 0.25$ and 0.35, respectively, we observe a trend to negative values at large p_t, which is in agreement with our earlier result.

Another striking feature is the breakdown of the polarization above $p_t = 1.2$ GeV/c at all x_F. This has not

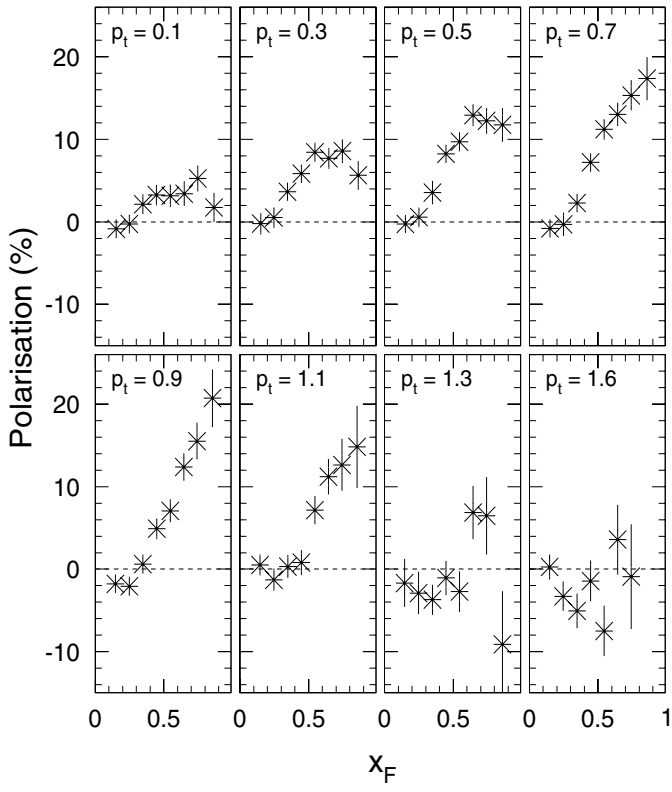

Fig. 6. Polarizations (in units of %)as a function of x_F for fixed bins in p_t. The mean values of p_t are indicated (in units of GeV/c)

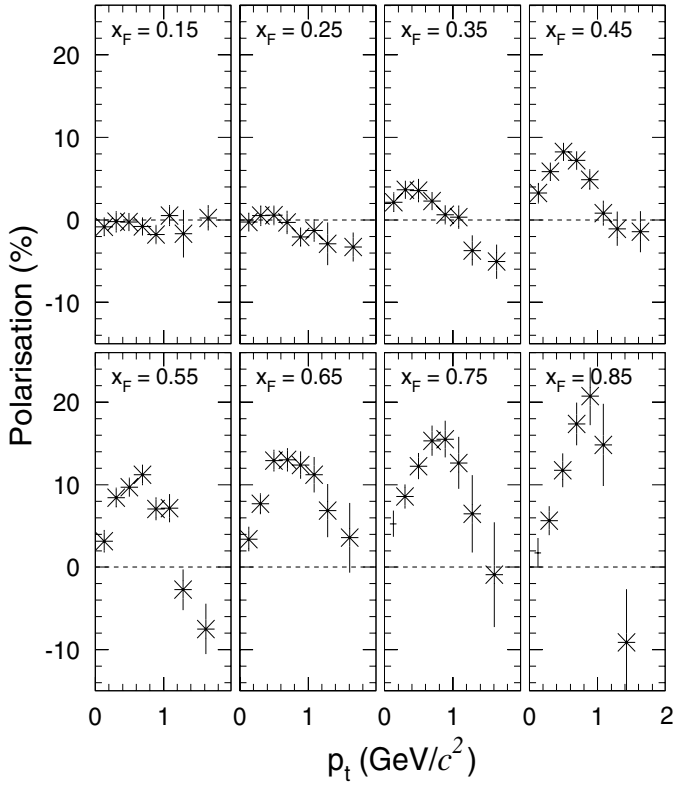

Fig. 7. Polarizations (in units of %) as a function of p_t (in units of GeV/c) for fixed bins in x_F. The mean values of x_F are indicated

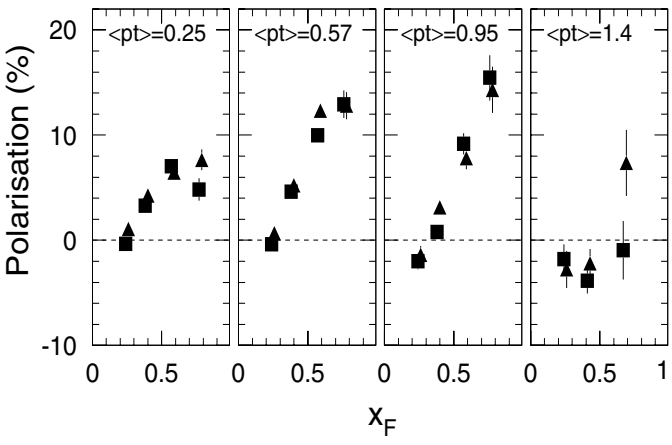

Fig. 8. Polarizations as a function of x_F for fixed intervals of p_t. Squares: Cu target, triangles: C target

been seen in *inclusive* Λ production by protons or neutrons, where the measurements extended to p_t values beyond 2 GeV/c . In the *exclusive* production process $pp \to p_f(\Lambda K^+)$, however, there is even a complete sign reversal of the polarization at $p_t(\Lambda) \approx 0.7$ GeV/c , as observed in a proton beam of 800 GeV/c at Fermilab [40]. In *inclusive* Σ^+ production by protons of 800 GeV/c , a less striking decrease of the polarization from +16% at $p_t = 1$ GeV/c to +12% at 1.5 GeV/c has been found [18].

Could the breakdown effect observed in our experiment have been produced in a secondary process rather than in the primary $\Sigma^- N$ interaction? In that case, we would expect a significant difference between production in the Cu target and in the C target, regardless of whether the secondary interaction took place in the same nucleus or in another nucleus further downstream. We do, indeed, observe at lower x_F a widenening of the p_t spectrum of the Λ produced in the copper target w.r.t. those produced in carbon. The polarizations themselves, however, show no systematic Cu/C difference as discussed above (see Fig. 8). Therefore we believe that secondary interactions cannot be the cause of the polarization breakdown.

Our sample of Λ particles was produced either directly (including Λ resonances) or via Σ parents. Using the lead-glass calorimeter to identify $\Sigma^0 \to \Lambda\gamma$ decays we have found that about 20% of our Λ sample comes from these decays. We have also identified $\Sigma^{\pm}(1385) \to \Lambda\pi^{\pm}$ decays. The fraction of Λs from $\Sigma^-(1385)$ and $\Sigma^+(1385)$ in the total sample is about 15% and 8% , respectively. Assuming the fraction from $\Sigma^0(1385)$ decays to be the mean of those two numbers, we find that about 35% of the Λ sample come from Σ^* decays, and thus more than half of the Λ sample was produced via Σ parent states. We do not observe a drastic change of this fraction with p_t.

Nevertheless it is tempting to speculate whether the surprising p_t dependence of the Λ polarization comes from different p_t dependences of the polarizations in inclusive Λ and inclusive Σ production.

Acknowledgements. It is a pleasure to thank J. Zimmer and G. Konorova for their support in setting up and running the experiment. We are also indebted to the staff of the CERN Omega spectrometer group for their help and support, to the CERN EBS group for their work on the hyperon beam line and to the CERN accelerator group for their continuous efforts to provide good and stable beam conditions. We also thank B. Friedgen of TU München for his help with preparing our final data tapes. Yu.A. Alexandrov gratefully acknowledges support by the Deutsche Forschungsgemeinschaft and the Russian Foundation for Basic Research under the contract number 436 RUS 113/465.

References

1. G. Bunce et al., Phys. Rev. Lett. **36**, 1113 (1976)
2. K. Heller et al, Phys. Rev. Lett. **41**, 607 (1978)
3. K. Heller et al., Phys. Rev. Lett. **51**, 2025 (1983)
4. B. Lundberg et al., Phys. Rev. D **40**, 3557 (1989)
5. E.J. Ramberg et al., Phys. Lett. B **338**, 403 (1994)
6. V. Fanti et al., Eur. Phys. J. C **6**, 265 (1999)
7. S. Erhan et al., Phys. Lett. B **82**, 301 (1979)
8. A.M. Smith et al., Phys. Lett. B **185**, 209 (1987)
9. A.N. Aleev et al., Eur. Phys. J. C **13**, 427 (2000)
10. S. Barlag et al., Phys. Lett. B **325**, 531 (1994)
11. S. A. Gourlay et al., Phys. Rev. Lett. **56**, 2244 (1986)
12. R. Rameika et al., Phys. Rev. D **33**, 3172 (1986)
13. J. Duryea et al., Phys. Rev. Lett. **67**, 1193 (1991)
14. D.M. Woods, Phys. Rev. D **54**, 6610 (1996)
15. Y.W. Wah et al., Phys. Rev. Lett. **55**, 2551 (1985)
16. C. Wilkinson et al., Phys. Rev. Lett. **58**, 855 (1987)
17. A. Morelos et al., Phys. Rev. Lett. **71**, 2172 (1993)
18. A. Morelos et al., Phys. Rev. D **52**, 3777 (1995)
19. K.B. Luk et al., Phys. Rev. Lett. **70**, 900 (1993)
20. A. Brandt et al., Nucl. Phys. B **519**, 3 (1998)
21. P.M. Ho et al., Phys. Rev. Lett. **65**, 1713 (1990) and Phys. Rev. D **44**, 3402 (1991)
22. B. Andersson et al., Physics Reports **97**, 31 (1983)
23. T.A. DeGrand and H.I. Miettinen, Phys. Rev. D **23**, 1227 (1981), **24**, 2419 (1981)
24. M. Anselmino et al., hep-ph/0008186v1
25. J. Félix, Mod. Phys. Lett. A **12**, 363 (1997)
26. A. Bravar, Proc. Conf. High energy spin physics, Protvino 1998, 167
27. J. Félix, Mod. Phys. Lett. A **14**, 827 (1999)
28. J. Soffer, hep-ph/9911373 (1999)
29. V.V. Abramov, hep-ph/0111128 (2001)
30. J. Félix, Mod. Phys. Lett. A **16**, 1741 (2001)
31. M.I. Adamovich et al., Z. Physik A **350**, 379 (1995)
32. Y. Yamamoto, K. Okubo and H. Toki, Prog. Theor. Phys. **98**, 95 (1997)
33. Liang Zuo-tang and C. Boros, Phys. Rev. Lett. **79**, 3608 (1997)
34. Yu.A. Alexandrov et al., Nucl. Instr. Meth. A **408**, 359–372 (1998)
35. W. Beusch, CERN/SPSC/77-70
36. W. Brückner et al., Nucl. Instr. Meth. A **313**, 345 (1992)
37. The Particle Data Group: K. Hagiwara et al., Phys. Rev. D **66** (2002)
38. M.I. Adamovich et al., Eur. Phys. J. C **26**, 357 (2003)
39. R.T. Edwards et al., Phys. Rev. D **18**, 76 (1978)
40. J. Félix et al., Phys. Rev. Lett. **88**, 061801 (2002)